

# Explaining the $L_x \sim L_{bol}$ Scaling for Massive-Star X-rays by Thin-Shell Mixing of Embedded Wind Shocks in the Radiative Limit

Stan Owocki & Jon Sundqvist

DRAFT NOTES, version of April 23, 2011

## 1. Introduction

Spurred by our recent discussions, and somewhat obliquely by Ken's recent emails and notes (which I still have not fully studied), I decided to write up some notes on ways to include radiative cooling effects in our semi-empirical models of X-ray emission. To give a specific focus, I decided to revisit the issue of how to explain the standard  $L_x \sim L_{bol}$  scaling law that has long been inferred empirically for massive stars, with the most recent re-affirmation coming in the paper by Naze et. al. analyzing the Chandra Carina data.

As far as I know, the only serious attempt to explain this scaling in terms of the basic Embedded Wind Shock (EWS) scenario is from the Owocki and Cohen (1999) analysis. Assuming a standard  $\rho^2$  emission, that analysis was able to obtain a *sublinear* scaling of  $L_x$  vs.  $\dot{M}/v_\infty$  by including the effects of b-f absorption in optically thick winds that had a power-law variation in the X-ray volume filling factor  $f_v$ .

Since in CAK theory,  $\dot{M} \sim L_{bol}^{1/\alpha}$ , with  $\alpha \approx 0.6$ , it had seemed that such a sublinear scaling of  $L_x \sim \dot{M}^\alpha$  might be necessary to give  $L_x \sim L_{bol}$ . However, as outlined in §3, Jon and I have been looking at ways that a linear scaling of  $L_x$  vs.  $\dot{M}/v_\infty$  could also give  $L_x \sim L_{bol}$  if one also accounts for a general scaling of luminosity with mass, e.g.  $L_{bol} \sim M^2$ .

Before getting to that, the analysis in the next section first generalizes the OC99 approach by accounting for radiative cooling through a new emission form that bridges the limits between the previous effective assumption of adiabatic expansion with the high-density limit of strong radiative cooling. For optically thick winds, this confirms the previous OC99 results of a potentially sublinear  $\dot{M}/v_\infty$  scaling for  $L_x$ , showing that it can indeed also be obtained in the case with strong radiative cooling.

However, for the perhaps more realistic assumption that the wind-absorption is generally quite weak (i.e.  $\tau_*$  order unity or less), we find a strictly *linear*  $\dot{M}/v_\infty$  scaling for radiatively cooled shocks (even with a power-law variation of heating with radius), recovering then the standard quadratic scaling  $L_x \sim (\dot{M}/v_\infty)^2$  in the limit of optically thin X-rays from adiabatically cooled shocks. The latter likely applies to B main sequence stars, and so explains the fact that they generally have  $L_x$  that falls well below the standard  $L_x \approx 10^{-7} L_{bol}$

found for the stronger winds of O stars and B supergiants. The former might explain this stronger wind scaling if we account for the mass-dependence of the luminosity.

## 2. Parameter Scalings for X-ray Emission from Embedded Winds Shocks

### 2.1. Bridging Law for Adiabatic vs. Radiative Emission

To begin, let us write the total X-ray luminosity as a general volume integral of (possibly b-f attenuated) X-ray emission,

$$L_x = \int \eta e^{-\tau} dV, \quad (1)$$

where the local emissivity scales as

$$\eta = f_v C \rho^2. \quad (2)$$

Here  $\rho$  is the wind density,  $C$  is a constant that depends on the shock model and atomic physics, and  $f_v$  represents a volume filling factor for X-ray emission.

While previous work has often directly parameterized this factor as following some power-law scaling with radius, e.g.  $f_v \sim r^{-q}$ , in the present notes we wish to account for the effect of radiative cooling, which is presumed to occur over some characteristic cooling length that scales as,

$$\ell = \frac{m_c}{\rho} \equiv \frac{1}{\kappa_c \rho}. \quad (3)$$

Here the cooling mass column  $m_c$  depends on the energy of the embedded wind shocks, and  $\kappa_c = 1/m_c$  provides a convenient representation with units of opacity or mass-absorption coefficient, i.e.  $\text{cm}^2/\text{g}$ . In the simple model here, we assume that the shock energy is fixed, and thus that  $\kappa_c$  is spatially constant. From eqns. (18) and (22) of Antokhin et al. (2003), we find a numerical value

$$\kappa_c = 190 E_{kev}^{-2} \text{cm}^2/\text{g}, \quad (4)$$

where  $E_{kev}$  is the shock energy in keV.

If this cooling length is *long* compared to the local radius, i.e. if  $\ell \gg r$ , then we may neglect radiative cooling, and simply compute the total X-ray luminosity in terms of the volume-integrated X-ray emission measure, as done in much (most) past work.

But if this cooling length is *short* compared to the local radius, i.e. if  $\ell \ll r$ , then we can expect that for some local “heating fraction”  $f_q$  (set by LDI-generated EWS), the resulting volume fraction  $f_v$  of X-ray emitting gas will be proportional to  $f_q$ , but locally *reduced* by a factor  $\ell/r$ .

To cover both asymptotic regimes, we may write a simple “bridging law” between the radiative and adiabatic cooling limits, yielding for the net volume filling factor,

$$f_v = \frac{f_q}{1 + r/\ell}, \quad (5)$$

which can be readily confirmed to yield the appropriate limits.

Applying these scalings, the volume emission integral becomes,

$$L_x = \int \frac{f_q \rho^2}{1 + \kappa_c \rho r} e^{-\tau} dV. \quad (6)$$

Within the bridging model, this form is quite general, and can even be applied to X-ray line emission if one includes a profile function in the integrand. We’ll return to this in §3.3, which shows line profiles Jon has computed for the radiative cooling limit. But for now, let’s explore how this model affects the scaling of  $L_x$  with  $\dot{M}$  and  $v_\infty$ .

## 2.2. Exospheric Scaling for Constant Speed Wind

To proceed, let us consider a simple “exospheric” scaling to account for any attenuation from the exponential absorption term,

$$L_x \approx 4\pi \int_{R_i}^{\infty} \frac{f_q \rho^2}{1 + \kappa_c \rho r} r^2 dr \quad (7)$$

with  $R_i \equiv \text{Max}[R_o, R_1]$ , where  $R_o$  is the *onset* radius for the X-ray emission, and  $R_1$  is the radius for unit radial wind optical depth, i.e.  $\tau(R_1) \equiv 1$ . Under the further simplification of a constant wind speed  $v = v_\infty$ , we have for bound-free (b-f) absorption opacity  $\kappa_{bf}$ ,

$$R_1 \equiv \frac{\kappa_{bf} \dot{M}}{4\pi v_\infty} \equiv \tau_* R_*. \quad (8)$$

In analogy with this unit-optical-depth radius, let us also define a characteristic radius for onset of adiabatic cooling,

$$R_a \equiv \frac{\kappa_c \dot{M}}{4\pi v_\infty}. \quad (9)$$

Let us further assume that the heating fraction has power-law scaling in radius

$$f_q(r) \equiv f_{qo} \left( \frac{R_o}{r} \right)^q. \quad (10)$$

Combining all these scalings, we find that emission integral now takes the form

$$L_x = 4\pi C_q \left[ \frac{\dot{M}}{4\pi v_\infty} \right]^2 \int_{R_i}^{\infty} \frac{1}{r + R_a} \frac{dr}{r^{1+q}}, \quad (11)$$

where, for notational simplicity, we defined a combined scaling constant  $C_q \equiv C f_{qo} R_o^q$ .

2.2.1. *Constant heating case in adiabatic and radiative limits*

For the radially constant heating case with  $q = 0$ , eqn. (11) integrates to

$$L_x = 4\pi C_q \left[ \frac{\dot{M}}{4\pi v_\infty} \right]^2 \frac{\ln[1 + R_a/R_i]}{R_a} \quad (12)$$

$$= \frac{C_q}{\kappa_c} \left[ \frac{\dot{M}}{v_\infty} \right] \ln[1 + R_a/R_i] \quad (13)$$

In interpreting this in terms of the overall scaling of  $L_x$  with  $\dot{M}/v_\infty$ , let's consider the various limits for the key radii  $R_a$  and  $R_i$ .

First, for optically thick winds with  $R_1 > R_o$  and thus  $R_i = R_1$ , note then that the ratio  $R_a/R_1 = \kappa_c/\kappa_{bf}$  is *independent* of  $\dot{M}/v_\infty$ , implying then a direct linear scaling,  $L_x \sim \dot{M}/v_\infty$ . Note this applies for both the radiative ( $R_a \gg R_o$ ) and adiabatic ( $R_a \ll R_o$ ) wind limits.

For optically thin winds, with  $R_1 < R_o$  and thus  $R_i = R_o$ , the ratio  $R_a/R_i = R_a/R_o$  now scales in proportion to  $\dot{M}/v_\infty$ . For radiative shocks with  $R_a \gg R_o$ , this now gives an additional logarithmic dependence on  $\dot{M}/v_\infty$ ; but since this is weak, the overall scaling is still roughly linear,

However, for optically thin, adiabatic winds – with both  $R_1 \ll R_o$  and  $R_a \ll R_o$  –, the expansion of the  $\ln(1 + R_a/R_o)$  in small  $R_a/R_o$  gives now an additional factor proportional to  $R_a \sim \dot{M}/v_\infty$ , recovering then the overall quadratic scaling  $L_x \sim (\dot{M}/v_\infty)^2$  that is characteristic of emission from shocks cooled by adiabatic expansion.

To summarize, for a wind with spatially constant heating ( $q = 0$ ), we find

$$L_x \sim \left[ \frac{\dot{M}}{v_\infty} \right] \quad ; \quad R_1 \gg R_o \quad (14)$$

$$\sim \left[ \frac{\dot{M}}{v_\infty} \right] \log(\dot{M}/v_\infty) \quad ; \quad R_1 \ll R_o \ll R_a \quad (15)$$

$$\sim \left[ \frac{\dot{M}}{v_\infty} \right]^2 \quad ; \quad R_1, R_a \ll R_o. \quad (16)$$

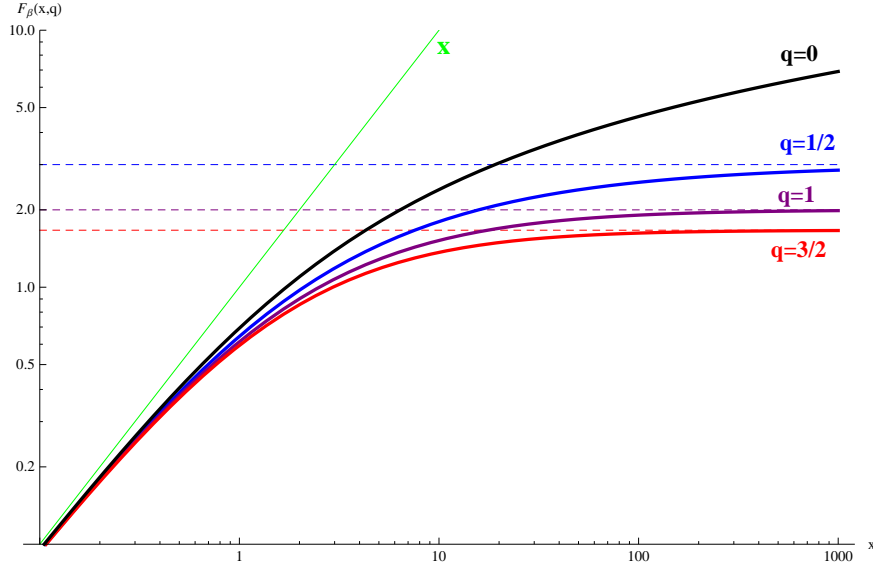


Fig. 1.— The modified-beta function  $F_\beta(x, q)$  vs.  $x$ , plotted on a log-log scale for  $q = 0, 1/2, 1$ , and  $3/2$ , as labelled. Note the linear scaling for small  $x \ll 1$  (cf. green line labeled “x”). For large  $x$ , the  $q = 0$  case diverges logarithmically, but other cases simply asymptote to a fixed values set by  $1 + 1/q$  (horizontal dashed lines).

### 2.2.2. Power-law heating case in adiabatic and radiative limits

More generally, for  $q \neq 0$  models that assume heating has a power-law variation in radius, we find

$$L_x = 4\pi C_q \left[ \frac{\dot{M}}{4\pi v_\infty} \right]^2 \frac{F_\beta[R_a/R_i, q]}{R_a R_i^q} \quad (17)$$

$$= \frac{4\pi C_q}{\kappa_c R_i^q} \frac{\dot{M}}{4\pi v_\infty} F_\beta[R_a/R_i, q]. \quad (18)$$

Here

$$F_\beta(x, q) \equiv \frac{|(-1)^q \beta(-x, q, 0)|}{x^q}, \quad (19)$$

where  $\beta$  is the incomplete beta function. Note that, for  $q = 0$ , this just recovers the logarithmic scaling of eqn. (13), i.e.,  $F_\beta(x, 0) = \log(1 + x)$ .

For selected representative values  $q = 0, 1/2, 1$ , and  $3/2$ , figure 1 plots the variation of  $F_\beta$  vs. argument  $x$  on a log-log scale. Note that the variation is linear at small  $x$ , and for

$q \neq 0$  just approaches a constant for large  $x$ ,

$$F_\beta(x, q) \approx x \quad ; \quad x \ll 1 \quad (20)$$

$$\rightarrow 1 + \frac{1}{q} \quad ; \quad x \gg 1, \quad q \neq 0. \quad (21)$$

We can readily apply these limits to derive power-law-heating scalings for  $L_x$  for optically thick vs. thin winds, and for radiative vs. adiabatic shock emission.

For optically thick winds, we again have  $R_i = R_1 \sim \dot{M}/v_\infty$ , so that eqn. (18) now gives a *sublinear* scaling for  $L_x \sim (\dot{M}/v_\infty)^{1-q}$ . This sublinear scaling was already found in the OC99 analysis of adiabatic shocks with power-law heating in an optically thick wind. But we now see that it applies equally well for both adiabatic and radiative shock emission.

For optically thin winds with an  $R_i = R_o$  that is independent of  $\dot{M}$ , the scaling from (18) again becomes linear for radiative shocks, but quadratic for adiabatic shocks.

So the summary scalings for power-law heating models with  $f_q \sim r^{-q}$  are thus:

$$L_x \sim \left[ \frac{\dot{M}}{v_\infty} \right]^{1-q} \quad ; \quad R_1 \gg R_o \quad (22)$$

$$\sim \left[ \frac{\dot{M}}{v_\infty} \right] \quad ; \quad R_1 \ll R_o \ll R_a \quad (23)$$

$$\sim \left[ \frac{\dot{M}}{v_\infty} \right]^2 \quad ; \quad R_1, R_a \ll R_o. \quad (24)$$

### 3. Implications for Observed $L_x/L_{bol}$ Scaling

#### 3.1. Numerical estimates for $R_a$ and $R_1$

Let us next estimate numerical values for the adiabatic radius  $R_a$  in terms of assumed wind parameters  $\dot{M}$  and  $v_\infty$ . Applying eqn. (4) into eqn. (9), we find

$$\frac{R_a}{R_*} = 140 \frac{\dot{M}_6}{E_{kev}^2 V_{1000} R_*/R_\odot}, \quad (25)$$

where  $\dot{M}_6 \equiv \dot{M}/10^{-6} M_\odot/\text{yr}$  and  $V_{1000} \equiv v_\infty/1000 \text{ km/s}$ . For example, for  $\zeta$  Puppis with  $\dot{M}_6 \approx 3$ ,  $V_{1000} \approx 2.5$ , and  $R_*/R_\odot \approx 20$ , and using the observed X-ray energy to estimate  $E_{kev} \approx 0.5$ , we find  $R_a \approx 33 R_*$ .

In next considering the unit-optical-depth radius  $R_1$ , it is important to note that b-f absorption has a similar inverse-square energy dependence, though now for the *photon* (vs. shock) energy. But if we assume these two energies have some fixed ratio,  $E_s/E_\gamma$ , then the ratios  $\kappa_{bf}/\kappa_c = R_1/R_a$  will also be fixed constants, with some characteristic value.

To estimate this value, let us consider results from the Cohen et al. (2010) analysis of X-ray line emission from  $\zeta$  Puppis. From fig. 12 of that paper, we can estimate that, for the ca. factor 2 reduction in CNO abundances (and taking  $E_\gamma = E_s$ , the b-f absorption opacity (averaged over edges) is approximately a factor  $\kappa/\kappa_c = 1/8$  smaller than this effective opacity for cooling. (For standard solar abundances, the reduction would perhaps be a factor 1/4.)

As a check, note for example that this implies lines near  $\sim 1$  keV in  $\zeta$  Pup have  $\tau_* = R_1/R_* \approx 1.5$ , in agreement with results in fig. 13 of Cohen et al. (2010).

### 3.2. Link between $L_x \sim \dot{M}/v_\infty$ and $L_x \sim L_{bol}$

Since the wind of  $\zeta$  Pup is among the strongest of all O-stars, we can anticipate that most of the stars observed for the standard  $L_x \approx 10^{-7} L_{bol}$  empirical law are typically quite optically thin, i.e.  $R_1 < R_o$ . However, the factor 4-8 higher values for  $R_a$  imply that these stars should generally have  $R_a > R_o$ , and so follow the *radiative* forms for shock emission.

As such, the relevant predicted scaling for O-stars should be the *linear* mass-loss relation given in eqn. (23), switching then to the steeper, quadratic scaling (24) for lower mass B-stars.

To connect from  $\dot{M}$  to  $L_{bol}$ , let us use the CAK scaling relation

$$\dot{M} \sim L_{bol}^{1/\alpha} M^{1-1/\alpha}, \quad (26)$$

where  $M$  is the stellar mass. Using also the scaling  $v_\infty \sim v_{esc} \sim \sqrt{M/R_*}$ , we find

$$L_x \sim \frac{\dot{M}}{v_\infty} \sim L_{bol}^{1/\alpha} M^{1/2-1/\alpha} \sqrt{R_*} \quad (27)$$

If we take a stellar structure scaling  $L_{bol} \sim M^s$ , then, ignoring for now the  $\sqrt{R_*}$  factor, we find

$$\log(L_x) \sim \frac{\alpha + 2s - 2}{2\alpha s} \log(L_{bol}). \quad (28)$$

To reproduce the empirical  $L_x \sim L_{bol}$  relation, we thus require

$$s = \frac{2 - \alpha}{2 - 2\alpha}. \quad (29)$$

For the standard CAK power index  $\alpha = 2/3$ , this requires  $s = 2$ , which actually is not an unreasonable mass-luminosity scaling for massive stars.

So this seems somewhat promising. But it really needs to be tested by seeing if the linear-wind-density scaling given in (27) might actually also give a acceptable, or perhaps even a tighter, fit to the observed  $L_x$ .

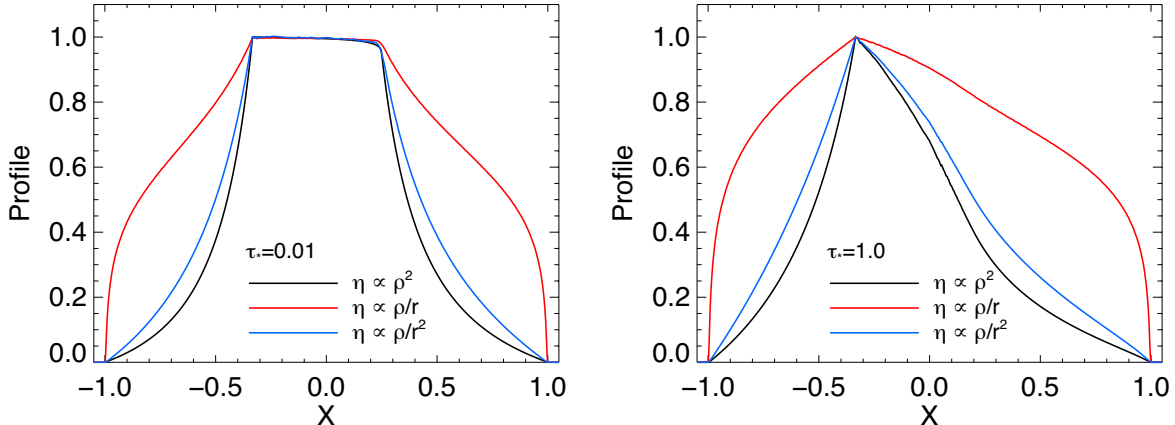


Fig. 2.— X-ray line profiles, overplotted for various models and parameters, as labelled.

### 3.3. Effect on X-ray Line Profiles

Upon showing this analysis to Jon, he offered to implement the new emission scaling in his X-ray line-profile code. Figure 2 compares results for the adiabatic (black) and radiative (red) limits for shock emission with a spatially constant heating, i.e.  $q = 0$ . The left and right panels are respectively for optically thin ( $\tau_* = 0.01$ ) vs. and marginally thick ( $\tau_* = 1$ ) line. The effect is quick striking, with the radiative emission (red curves) much broader, due the weaker radial decline implied by the  $\rho$  vs.  $\rho^2$  scaling.

Recall that previous models with  $\rho^2$  generally give quite good fits to observed lines without invoking any radial variation in the X-ray volume filling factor, i.e.  $f_v = \text{constant}$ . Thus we can certainly rule out such radiative shock models with  $q = 0$ .

But note the blue curve that shows a corresponding radiative model with  $q = 1$ , i.e. with shock heating that declines as inverse radius after the shock onset,  $f_q \sim 1/r$ . This is actually very close to the adiabatic, constant filling factor models shown in black, and so would presumably also provide a quite good fit to observed line-profiles!



Indeed, one can readily see that the adiabatic  $q = 0$  model and the radiative  $q = 1$  models have very similar radial scalings for the emissivity. Specifically, their ratio differs simply by the scaled velocity law,  $\eta_{rad}(r, q = 1)/\eta_{ad}(r, q = 0) = w(r) = v(r)/v_\infty$ .

Bottom line: the radiative model with  $q = 1$  provides a more physically appropriate alternative to the previous adiabatic,  $q = 0$  approach. Moreover, the linear vs. quadratic scaling of such radiative model with  $\dot{M}/v_\infty$  provides a possibility of reconciling with the empirical scaling  $L_x \sim L_{bol}$ , if one assumes a mass-luminosity relation  $L_{bol} \sim M^s$  with  $s \approx 2$ .

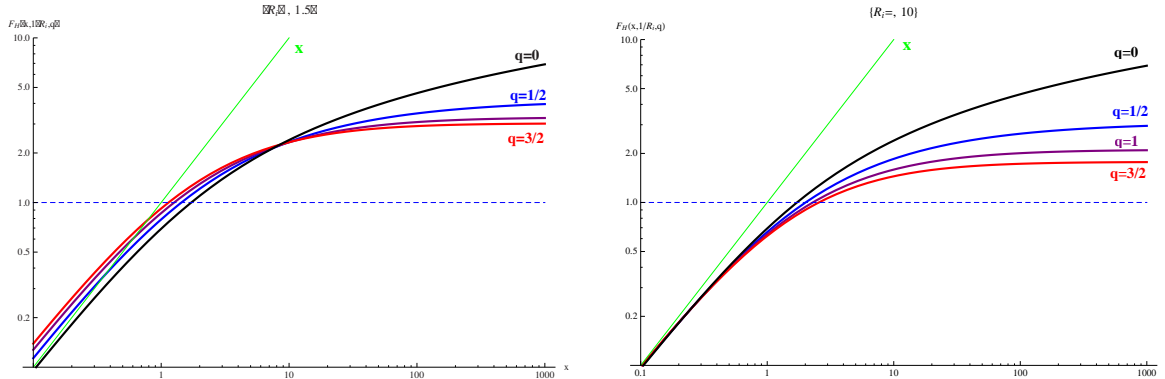


Fig. 3.— The function  $F_H(x, y, q)$  vs.  $x$ , plotted on a log-log scale for  $q = 0, 1/2, 1$ , and  $3/2$ , as labelled. The left and right panels are for respectively  $y = R_*/R_i = 2/3$  and  $y = 1/10$ . The general behavior is very similar to that for the  $F_\beta$  function introduced in the above constant-wind-speed analysis, and plotted in figure 1; namely it is linear for small  $x \ll 1$  (cf. green line labeled “x”), and asymptotically constant ( $q > 0$ ) or logarithmically divergent ( $q = 0$ ) for large  $x$ .

#### 4. Addendum from 17Apr11: Effect of Wind Velocity Law

The above scaling analysis assumes, for simplicity, a constant wind speed. But we can also readily examine the effect of including a wind velocity law assuming the standard  $\beta = 1$  form,

$$w(r) \equiv \frac{v(r)}{v_\infty} = 1 - R_*/r. \quad (30)$$

Application in eqn. (7) shows that the emission integral for the power-law heating case (cf. eqn. (11)) now takes the form,

$$L_x = 4\pi C_q \left[ \frac{\dot{M}}{4\pi v_\infty} \right]^2 \int_{R_i}^{\infty} \frac{r^{-q}}{r - R_* + R_a} \frac{dr}{r - R_*}. \quad (31)$$

Direct integration now yields

$$L_x = \frac{4\pi C_q}{\kappa_c R_i^q} \left[ \frac{\dot{M}}{4\pi v_\infty} \right] \frac{F_H[R_a/(R_i - R_*), R_*/R_i, q]}{1 + q}, \quad (32)$$

where

$$F_H[x, y, q] \equiv \ln[1 + x] \quad ; \quad q = 0 \quad (33)$$

$$\equiv \frac{{}_2F_1[1, q, 1 + q, y] - {}_2F_1[1, q, 1 + q, y(1 + x) - x]}{q/(1 + q)} \quad ; \quad q > 0, \quad (34)$$

with  ${}_2F_1$  the Hypergeometric function.

Compared to the function  $F_\beta$  defined in eqn. (21), this  $F_H$  function has somewhat difference arguments, depending separately now on  $y = R_*/R_i$  as well as a modified adiabatic radius ratio  $x = R_a/(R_i - R_*)$ . But for any  $y$ , the overall behavior vs.  $x$  is quite similar to the  $F_\beta(x, q)$  derived for the constant-wind-speed case, including the linear variation at small  $x \ll 1$ , and the asymptotically constant (for  $q > 0$ ) or logarithmic (for  $q = 0$ ) scaling for large  $x \gg 1$ . Figure 3 illustrates this explicitly for both optically thin ( $R_i = R_o = 1.5R_*$ ; left panel) and optically thick winds ( $R_i = R_o = 10R_*$ ; right panel).

Given this, and noting the essentially identical forms of eqns. (18) and (31), we thus conclude that inclusion of a velocity law does not change the overall  $L_x$  scalings shown in eqns. (22) – (24). In practice, for most O-star winds, we thus again expect the linear scaling given in eqn. (23), with then the same prospects as developed above for explaining empirical  $L_x$  vs.  $L_{bol}$  scalings.

## 5. Addendum from 21Apr11: Effect of Shock Mixing

The inherent thinness of radiative shock cooling zones makes them subject to various thin-shell instabilities. These can be expected to lead to an unknown level, but potentially substantial, level of *mixing* between cool and hot material, Since cooler material radiates more efficiently, and in softer wavebands toward to UV vs. X-rays, such mixing could significantly *reduce* the effective emission of X-rays. While there have been some numerical simulations of the complex structure that can arise from instabilities (e.g. Walder & Folini (1998, A&A 320, L21-L24), there unfortunately does not appear to be any detailed study of how this can effect the net X-ray emission.

To examine the potential effect of such mixing on X-ray scalings, let us make the plausible ansatz that the reduction should, for shocks in the radiative limit  $\ell/r \ll 1$ , scale as

some power of the ratio of the cooling length ratio,  $\ell/r$ , To ensure that the mixing effect goes away in the adiabatic limit, we can assume a similar ‘bridging law’ scaling for an “mixing reduction factor” for X-rays,

$$f_{xm} = \frac{1}{(1 + r/\ell)^m}, \quad (35)$$

where  $m > 0$  is some “mixing power index”. To account for mixing with this model, we thus simply multiply the integrand for X-ray emission by this factor.

To write a fully general form, let us consider yet one more generalization to our model. Namely, let us also allow for the possibility that the X-ray onset may not be as a step function, but rather increases itself as some power  $s$  of the scaling wind speed,  $w(r) = v(r)/v_\infty$ , while still possibly declining outward as radial power  $q$ ,

$$f_q(r) = f_{qo} H[r - R_o] [w(r)]^s \left[ \frac{r}{R_o} \right]^q, \quad (36)$$

where  $H(x)$  is the Heavidside step function, with unit value for postive  $x$ , and zero otherwise.

With these two further added power scalings, we can write the X-ray emission integral in the (perhaps too?) general form,

$$L_x = 4\pi C_q \left[ \frac{\dot{M}}{4\pi v_\infty} \right]^2 \int_{R_i}^{\infty} \frac{dr}{r^{q+s} (rw + R_a)^{1+m} (rw)^{1-m-s}}. \quad (37)$$

Note that for the  $\beta = 1$  velocity assumed in eqn. (30), we have  $rw = r - R_*$ ; thus for  $\beta = 1$  and  $m = s = 0$ , we simply recover eqn. (31).

Indeed, for  $\beta = 0$  and thus  $w = 1$ , we recover for  $s = m = 0$  the constant-wind-speed scaling of eqn. (11).

But, as written, eqn. (37) even allows us now also to account for non-unit values of the  $\beta$  velocity index. So far I’ve only been able to find analytic expressions for the  $\beta = 1$  case, which for general values of  $q$ ,  $s$ , and  $m$  turns out to involve yet another obscure function (the “Appell Hypergeometric function”). Evaluation turns out to be quite tricky though, and so I’ve found it simpler just to evaluate the integral numerically.

Inspection of (37) shows that the  $R_a$  term sets the length scale of the integrand, so that in the radiative shock limit  $R_a \gg R_i$ , we can extract a  $1/R_a^{1+m}$  factor that now makes the mass-loss-rate scaling potentially *sublinear*,  $L_x \sim (\dot{M}/v_\infty)^{1-m}$ . Once this overall factor is extracted, the remaining integral function again just follows a simple “bridging” behavior between the radiative ( $R_a \gg R_o$ ) and adiabatic ( $R_a \ll R_o$ ) limits.

As a specific example, let us consider the relevant case of an optically thin wind ( $R_I = R_o = 1.5R_*$  with an inverse radius decline in heating ( $q = 1$ ), but now with various  $s$  and mixing exponents  $m$ . The integral turns out to have the form

$$L_x = 4\pi C_q \left( \frac{\dot{M}}{4\pi v_\infty} \right)^2 \frac{1+m}{\sqrt{1+s}} \frac{F_m[R_a]}{R_a^{1+m}} \quad (38)$$

$$\approx \frac{4\pi C_q}{\kappa_c^{1+m}} \left[ \frac{\dot{M}}{4\pi v_\infty} \right]^{1-m} \frac{1+m}{\sqrt{1+s}} \frac{R_a}{R_a + 1/(1+s)/(1+m)^3}, \quad (39)$$

where the latter approximation follows from full numerical integration.

For example, figure 4 overplots  $F_m(x)$  vs.  $x \equiv (1+s)(1+m)^3 R_a$  for select values of  $m$ , for both  $s = 0$  (left) and  $s = 1$  (right). The clearly shows the very good fit to the simple bridging law  $F_m(x) \approx x/(1+x)$ , plotted as the black curve.

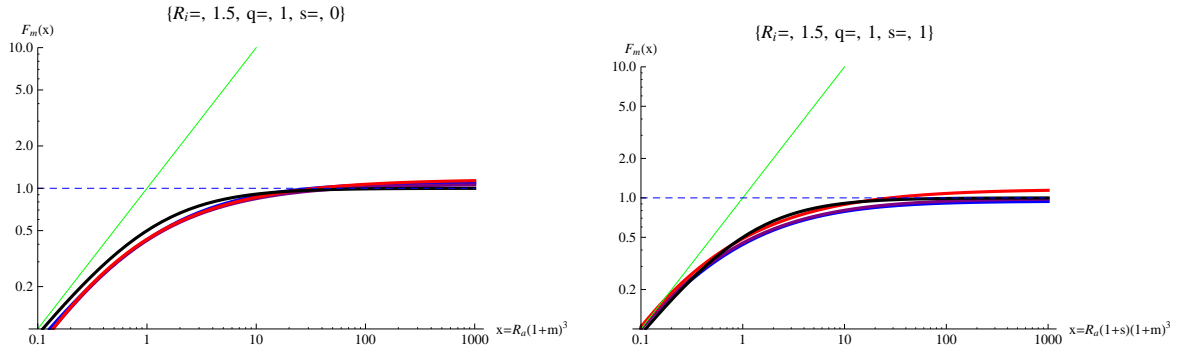


Fig. 4.— Numerical integration plot for  $F_m(x)$  vs.  $x = (1+s)(1+m)^3 R_a$  for cases with velocity-dependent heating exponent  $s = 0$  (left) and  $s = 1$  (right), overplotted for selected values of the mixing exponent  $m=0, 0.2, 0.4$  (blue, purple, red). The black curve represents the simple bridging law  $x/(1+x)$ . This bridging behavior is very similar to that for the  $F_\beta$  and  $F_h$  functions introduced in previous models; namely it is linear for small  $x \ll 1$  (cf. green line labeled “x”), and asymptotically constant for large  $x$ .

Bottom line: for  $m > 0$  this mixing effect can lead to a *sublinear* scaling of the X-ray luminosity with the mass-loss rate,  $L_x \sim (\dot{M}/v_\infty)^{1-m}$ .